Metallography, Microstructure, and Analysis
https://doi.org/10.1007/s13632-024-01103-z

ORIGINAL RESEARCH ARTICLE

Impact of Melt Thermal Treatment and Artificial Aging on Microstructure and Mechanical Properties of A356 Alloy

Sunil Manani[1] · **Mukesh Kumar**[1] · **Patel Nikunj**[1] · **Ajaya Kumar Pradhan**[1]

Received: 28 January 2024 / Revised: 12 June 2024 / Accepted: 11 July 2024

Abstract

This paper presents the individual and the combined impact of melt thermal treatment and artificial aging treatment on microstructure and mechanical properties of A356 alloy. Samples modified with and without strontium (Sr)-based master alloy are also prepared for comparison purposes. The as-cast results for melt thermal treatment processed alloys displayed the refinement of α-Al grains coupled with a drop in eutectic silicon length. Further treatment results of artificial aging treatment alter eutectic silicon morphology into a spherical shape, and distribution of α-Al and eutectic silicon phase improves significantly compared to as-cast A356 alloys. The best eutectic silicon modification in terms of aspect ratio and roundness is obtained in the case of aged A356 alloy processed through melt thermal treatment along with Sr modifier. Because of this improvement in eutectic Si characteristics, the ultimate tensile strength, elongation, and hardness of the aged A356 alloy treated through melt thermal treatment along with Sr modifier increased by 9.6%, 24.4%, and 10.1%, respectively, compared to the aged untreated alloy. DSC results show that a maximum shift in eutectic peak temperature is observed in the melt thermal treatment along with Sr modifier A356 alloy.

Keywords Melt thermal treatment · Eutectic Si · A356 alloy · Modifier · As-cast · Aged

Introduction

Among different hypoeutectic Al–Si–Mg alloys, A356 series alloys are most commonly used by industries because of their relatively high strength to weight ratio and low cost. As-cast A356 alloys consist of coarse α-Al dendrites and needle-like eutectic silicon, which negatively affects the mechanical properties of the alloy such as tensile strength, hardness, toughness, and ductility. These properties can be improved by grain refinement of α-Al dendrites and by modifying eutectic silicon shape from acicular to spheroidal [1–3].

Traditionally, grain refinement can be achieved by chemical treatment such as the addition of Al–Ti–B- or Al–Ti–C-based master alloys [4–8] and by mechanical treatment such as ultrasonic vibration treatment [9–11]. It is well known that the grain refining efficiency of a refiner depends on the effective heterogeneous nucleation sites provided by the refiner. All these refining techniques have their limitations. For example, Ti-based refiner (e.g., Al–Ti–B) undergoes decreased grain refining efficiency when added to Al–Si (Si > 5 wt%) melts because of the Si poisoning effect. According to this effect, many of the nucleation particles such as AlTi3 or TiB2 formed from Ti-based refiners get coated with Al-Ti-Si compounds [12, 13], which reduces the number of effective nucleation sites for aluminum dendritic formation. Similarly, Taghavi et al. [9] reported that the complexity of the required equipment and overall high cost of the ultrasonic vibration method makes it difficult to accept in actual industrial practice.

The eutectic silicon particle characteristics such as roundness, aspect ratio, etc., affect the mechanical properties, in particular ductility of Al–Si alloy. Various modification techniques can control the size and shape of eutectic Si. Several investigators [1, 14–17] have reported that the eutectic Si shape can be changed from needles to fibrous by adding a small amount of Sr and mischmetal (MM) such as Ce- and

This invited article is part of a special topical focus in the journal *Metallography, Microstructure, and Analysis* on Quantitative Metallography and Microstructure Modeling.

✉ Ajaya Kumar Pradhan
ajaya.meta@mnit.ac.in

1 Department of Metallurgical and Materials Engineering, MNIT Jaipur, Jaipur 302017, India

Published online: 22 July 2024

Nb-based master alloy. Zhu et al. [14] have found that the percentage elongation increases by 10.25% by MM-modification along with T6 heat treatment in the case of A356 alloy.

Melt thermal treatment (MTT) is a modified casting process that causes refinement and modification of Al–Si melt structure without any additives. The concept of melt thermal treatment was first proposed by Banamove [18] and concluded that when a superheated melt and an undercooled melt of the same chemical composition are mixed, it creates many nucleation sites for the solidification of the primary phase. This treatment can reduce the size of the primary silicon in hypereutectic aluminum–silicon alloys [19, 20]. Wang et al. [21] have also observed that the primary Si refined to about 20 µm from about 50 µm, and the eutectic silicon modified by melt thermal treatment. Jia et al. [22] have reported that tensile strength and elongation increase by 20.3% and 19.2%, respectively, by the melt thermal rate treatment, compared to the untreated Al–9Si–0.5Mg alloy. Samuel et al. [23] have also reported that strontium modification along with melt thermal treatment leads to better tensile properties and eutectic silicon modification than only strontium modification in A356 alloy.

In refined and modified alloys, eutectic Si distribution is usually heterogeneous, and the morphology is fibrous, which still needs improvement for better ductility. Age hardening treatments, including solutionizing followed by quenching and artificial aging, can optimize mechanical properties. These treatments result in a change of morphology of Si to spheroidal form in hypoeutectic Al–Si alloy. Various researches have been conducted [24–31] on chemical modification and T6 heat treatment's combined effect on Al–Si–Mg alloys. Zue et al. [31] studied on effect of T6 heat treatment on the microstructures, tensile properties of 356 alloy with and without modifier. It is observed that T6 treatment modified morphology of eutectic silicon particles. The influence on the degree of spheroidization of eutectic silicon particles is greatly for with modifier A356 alloys than that of without modifier alloy. However, minimal work is carried out to determine the combined impact of MTT and age hardening treatment on microstructure and mechanical properties. The aim of this paper is to investigate the combined impact of MTT and artificial aging on microstructure, thermal behavior, and mechanical properties of A356 alloy. The author selected shorter solution treatment and artificial aging time to study the effect on degree of spherodization of the eutectic Si of with and without MTT processed alloys.

Materials and Methods

In melt thermal treatment (MTT) process, commercial pure A356 alloy (procured from Kastwel foundries) was remelted in an electrical resistance furnace at 720 °C and was held at that temperature for 1 h for homogenization. The prepared melts were degassed using C_2Cl_6 tablet. Further, the prepared melts (with or without modifier) were divided in 1:1 ratio into two different graphite crucibles. One half of the melt, termed as high-temperature melt (HTM), was transferred to a furnace held at temperature 900 °C, and the other half melt termed as low-temperature melt (LTM) was transferred to a furnace held at temperature 600 °C. These HTM and LTM were held at their respective temperatures for 15 min, and then, the HTM melt was mixed with the LTM melt. Finally, the mixed melt was poured into a preheated (250 °C) cylindrical graphite mold (20 mm × 150 mm) for casting. In order to study the combined effect of modifier and MTT, a melt was also prepared by the addition Al–5Sr (Sr-200 ppm) modifier in the melt after degassing. Further, similar procedure of MTT was used as described above. These alloys termed as MTT processed alloys.

The A356 alloy (with or without modifier) was also prepared without the MTT process for comparison purposes. For this purpose, prepared melts (with or without modifier) were degassed by C_2Cl_6 tablet followed by pouring into a preheated cylindrical graphite mold. Such type of prepared alloys termed as conventionally processed alloys. Further, all the prepared alloys were solutionized at 550 °C for 120 min followed by quenching in hot water at 70 °C and then artificial aging at 175 °C for 150 min. Finally, the samples were air cooled. The cast alloys termed as as-cast alloy and heat treated (T6) corresponding alloys termed as aged alloy.

The chemical composition of A356 alloy and Al–5Sr master alloy as investigated by optical emission spectroscopy (OES) technique (Spectrolab) is listed in Table 1. Sample details and alloy code of various prepared alloys are listed in Table 2. A circular band cut all cast and aged samples perpendicular to the centerline axis of samples and were polished according to the standard metallographic procedure. The polished samples were then etched with Keller's etchant (95-ml H_2O + 2.5-ml HNO_3 + 1.5-ml HCl + 1-ml HF) for microstructural examination, and for macrostructural analysis, the samples were etched with Poulton's etchant (60-ml HNO_3 + 30-ml HCl + 5-ml HF + 5-ml H_2O). For microstructural observation, both the as-cast and heat-treated specimens were examined using a scanning electron microscope (FE-SEM, Nova Nano

Table 1 Chemical composition (wt%) of various procured alloys

Element	Si	Mg	Fe	Ti	Cu	Mn	Zn	V	B	Sr	Al
A356 alloy	6.81	0.32	0.15	0.03	0.05	0.05	0.01	0.01	–	–	Bal
Al–5Sr	0.1	0.01	0.24	0.006	0.001	0.004	0.001	0.012	–	4.82	Bal.

Table 2 Sample description of prepared A356 alloy under different casting conditions

Alloy code	Alloy description
A	Casting of A356 alloy via conventional casting process
MTT	Casting of A356 alloy via melt thermal treatment process
AM	Casting of (A356 + Al–5Sr) alloy via conventional casting process
MTTM	Casting of (A356 + Al–5Sr) alloy via melt thermal treatment

SEM 450). The macrostructure of the samples was observed using a stereomicroscope at 12X magnification. The parameters, i.e., mean diameter, aspect ratio, and roundness, used to characterize the size and shape factor of silicon particles in the samples were analyzed using Image Pro Plus 6.0 software.

Mean diameter is the average length of diameters measured at 2° intervals, the aspect ratio is the ratio between the major axis and minor axis of the particles, and roundness (R) is defined as $R = p^2/(4\pi S)$, where p and S represent the perimeter and area of a particle [31].

Differential scanning calorimeter (NETZSCH DSC 404 F3) analysis was carried out to identify changes in eutectic silicon peak temperature of A356 alloys after adding modifier and MTT. Small samples weighing 15–20 mg were cut and placed in an Al_2O_3 crucible under a nitrogen gas atmosphere with a 60 ml/min flow rate for analysis. The samples were heated up to 700 °C from room temperature and cooled to 300 °C at a rate of 10 °C/min during the measurement.

Tensile test was conducted on a universal testing machine (Model: H25KL, Tinius Olsen) at a strain rate of 1 mm/min. The testing was carried out on at least two different standard samples ((ASTM E08, gauge diameter = 6 mm and gauge length = 24 mm) prepared under similar conditions to ensure reproducibility of the results. Fracture analysis of tensile test specimens was carried out to relate the fracture mode and morphology of eutectic Si using a scanning electron microscope. Vickers microhardness (ASTM E384) was measured of at least two different samples prepared under identical conditions using a load of 200 g and a dwell time of 15 s, and an average of reading was considered.

Results and Discussion

Microstructural Analysis

As-Cast Alloys

Figure 1 shows the variation in macrostructure, and Fig. 2 shows variation in SEM microstructure of as-cast A356 alloy prepared by different methods. The macrostructures show that the MTT processed alloys (MTT and MTTM) consist of the refined and equiaxed grain structure of α-Al phase compared to conventionally processed alloys, with or without modifier (A and AM alloy). This is because of intermixing of HTM with LTM, which produced many nucleation sites for the solidification of α-Al phase. The maximum grain size reduction is observed in the MTTM alloy, which is ~50% compared to the A alloy. From SEM microstructure (Fig. 2), it is observed that prepared alloys microstructure consists of α-Al dendrites (plain black regions) and eutectic Si (white regions) in the form of needle-like in A and MTT alloys (Fig. 2a and b) and fibrous-like structure in AM and MTTM alloys (Fig. 2c and d). However, the size of the eutectic Si is lesser in the case of MTT alloys compared to A alloys without any other changes in morphology. In the case of Sr-modified alloys (AM and MTTM), the morphology of eutectic Si gets transformed into short rod-like and/or spherical shapes from needles-like shapes. When a modifier is added to the melt, the growth mechanism of eutectic Si changes, and is known as impurity-induced twinning. According to this mechanism, Sr modifier atoms segregate at the interface of solid dendrites and eutectic liquid, and inhibit the growth of eutectic Si particles.

Apart from them, intermetallic phase such as Fe-rich phase (marked by white circle in Fig. 2) is present in the form of Chinese script type and needle-like in each samples. EDS analysis (Fig. 2e) confirmed the presence of the Fe-rich phase in the microstructure of alloys.

Table 3 quantitatively shows variation in average grain size of α-Al (g) and eutectic Si particles length (l) of prepared alloys. It is observed that the α-Al grains get refined, and the average length of eutectic Si particles reduced significantly in both the MTT processed alloys. The percentage reduction in g and l in case of the AM alloy is appx. 41% and 32.2% than that of the A alloy, respectively. The average length of eutectic Si in MTTM alloy was reduced by appx. 86% and 14% compared to CC and MCC alloy, respectively. Similar observations have been made by Samuel et al. [23] and have reported that MTT exhibits refinement in eutectic Si to a certain extent without change in morphology. Wang et al. [32] have also concluded that the MTT process refines α-Al because of the multiplication of nucleation site for solidification of α-Al after intermixing.

According to Wang et al. [10, 11], intermixing of the HTM and the LTM forms many small and uniformly distributed solid-like atomic clusters in the final melt. These atomic clusters act as nucleation sites for α-Al phase. Also, LTM has semi-solid content, which when mixed with HTM produces free secondary dendritic arms. These free secondary

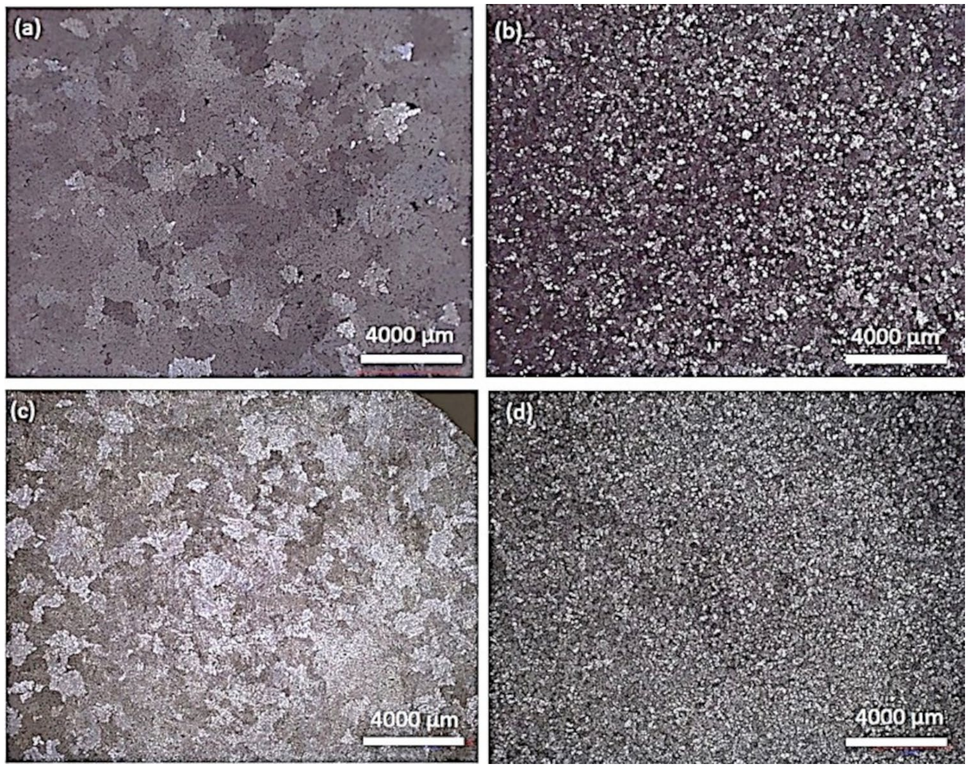

Fig. 1 Macrostructure of as-cast A356 alloys **a** A, **b** MTT, **c** AM, and **d** MTTM

dendritic arms also act as heterogeneous nucleation sites for α-Al. In both of the above-mentioned ways, MTT processed alloys (MTT and MTTM) produce finer microstructure (Fig. 1b and d).

Aged Alloys

The aging treatment causes spherodization of eutectic Si particles and precipitation of Mg_2Si in both unmodified and modified alloys [28, 29]. SEM microstructure of aged A356 alloy prepared under different casting conditions is presented in Fig. 3. The gray and black region in the microstructure indicates transformed eutectic Si and α-Al phase, respectively**.** In each alloy, aging treatment alters eutectic Si morphology into rounded shape, and distribution of both the phases (eutectic Si and α-Al) improves considerably compared to respective as-cast alloy. However, degree of spherodization and morphology of the eutectic Si are different in each alloys. The microstructure of alloy A consists of partially transformed eutectic Si in the form of rod/fibrous structure, and MTT alloy consists of coarse spheroids Si. Fine sized spheroids Si present in AM alloy and MTTM alloy. These indicate that degree of spherodization in with modifier alloys (AM and MTTM) is better than that of without modifier alloy (A and MTT) for short solutionizing time. However, large-sized and rod-like eutectic Si in the aged alloy A can be observed compared to MTT-treated alloy.

Table 4 quantitatively summarizes variations in eutectic Si characteristics after aging. The results indicate that MTT significantly reduced the mean diameter and aspect ratio compared to untreated A356 alloy (A). Since the average length of eutectic Si is lesser (~ 49%) in the case of as-cast MTT alloys than the as-cast A alloy, it leads to better spherodization in MTT alloys after aging. However, there is a less significant change in the MTT alloy's aspect ratio than the modified alloy. A minimum aspect ratio of 1.52 is observed in the case of the MTTM alloy. The maximum improvement in roundness is observed in MTTM (1.54) alloy as compared to the A alloy (3.71). These results reveal that the addition of modifier along with MTT treatment leads to best modification in the morphology of eutectic Si than only modifier addition or MTT treatment even at the short solutionizing time.

The reason behind these variations in microstructure is explained by Paray et al. [30] and Kahtani et al. [33]. According to them, there are mainly three stages through which the morphology of eutectic Si gets altered in aging treatment. In the first stage, large Si particles break into several small Si particles, followed by spherodization of eutectic Si. Then, if the solutionizing time is too large, the size of particles starts increasing, which is known as coarsening. In the present work, solutionizing time is short (120 min), leading to incomplete spherodization in the A alloy case. However, in the case of the modified alloys (AM and MTTM), the morphology of eutectic Si is already modified into the

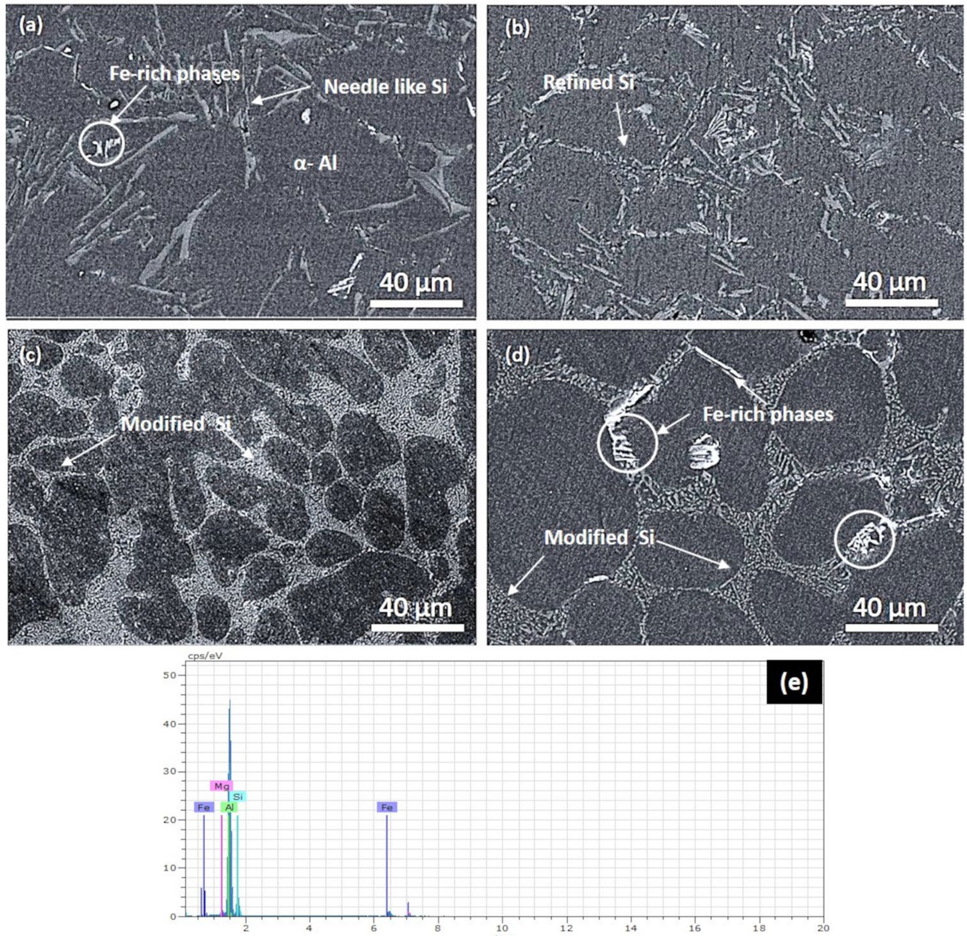

Fig. 2 SEM micrographs of as cast A356 alloys **a** A, **b** MTT, **c** AM, and **d** MTTM

Table 3 Quantitative variation in microstructural features of as-cast A356 alloys

Sample	Grain size (µm)	Eutectic Si length (µm)
A	730 ± 45	23.9 ± 5.3
MTT	425 ± 20	12.2 ± 2.7
AM	630 ± 25	3.2 ± 1.4
MTTM	365 ± 17	3.7 ± 2.1

fibrous structure in cast condition because of the addition of a modifier. This requires less time during the first stage of aging treatment than unmodified alloy and leads to complete spherodization.

DSC Analysis

The DSC cooling curves (cooling rate = 10 °C) of as-cast A356 alloys treated in various ways are shown in Fig. 4. These curves indicate that each alloy exhibits two exothermic peaks, one at higher temperature (between 615.76 and 605.6 °C) corresponding to solidification of α-Al dendrites and the other at a lower temperature (between 571.9 and 546.08 °C) corresponding to solidification of eutectic Al–Si.

Table 5 lists the liquidus temperature (T_l), solidus temperature (T_s), solidification range, and eutectic peak temperature (T_{ep}) of A356 alloys treated in various ways. The temperature of eutectic Al–Si is shifted to lower temperatures after adding modifiers in both AM and MTTM alloys. The maximum shift in eutectic peak temperature is observed in the MTTM alloy compared to the A alloy. The eutectic temperature shift is 2.44 °C, 4.9 °C, and 5.1 °C in MTT, GM, and MTTM alloys, respectively, compared to the A alloy. This indicates that the amount of required undercooling for solidification of the eutectic phase is higher in the case of MTTM alloy. Chen et al. [34] have also found that the Li-based modifier reduces the eutectic temperature of base A356 alloy and increases undercooling. Research by Kanga et al. [35] summarizes that a sufficient eutectic depression (at least 6 °C) is required for the morphology transition into the fibrous structure of eutectic Si crystals.

The DSC results show a significant increment in the solidification range (difference between liquidus and solidus

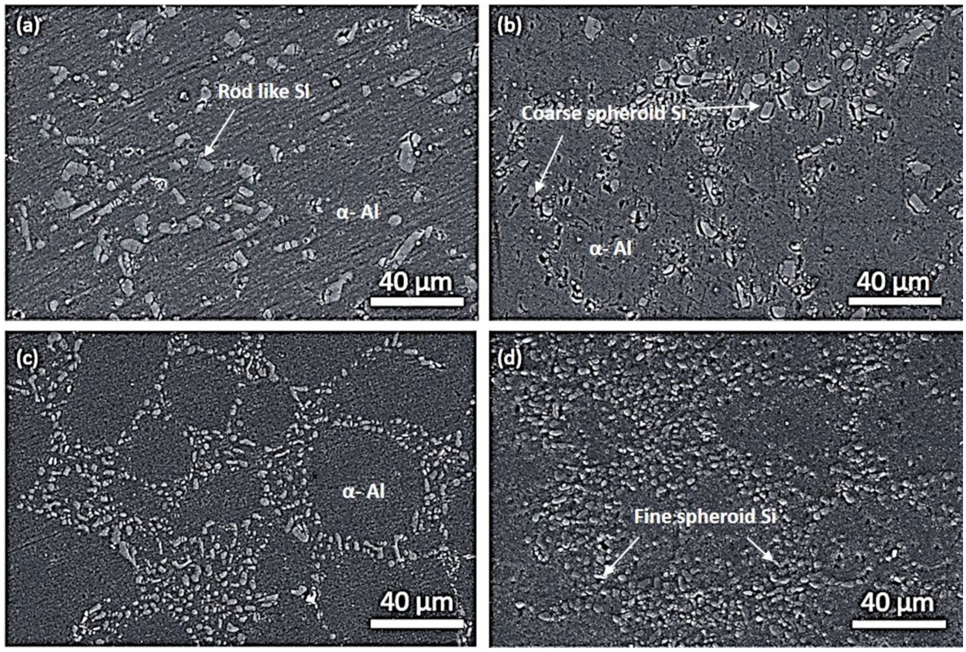

Fig. 3 SEM micrographs of aged A356 alloys **a** A, **b** MTT, **c** AM, and **d** MTTM

Table 4 Quantitative variation in eutectic Si characteristic of various aged A356 alloys

Sample	Diameter (µm)	Roundness	Aspect ratio
A	6.32 ± 2.25	3.71 ± 0.85	3.11 ± 1.2
MTT	4.71 ± 1.51	3.14 ± 0.57	2.41 ± 0.88
AM	2.15 ± 0.85	1.89 ± 0.53	1.75 ± 0.72
MTTM	1.87 ± 0.57	1.54 ± 0.35	1.52 ± 0.42

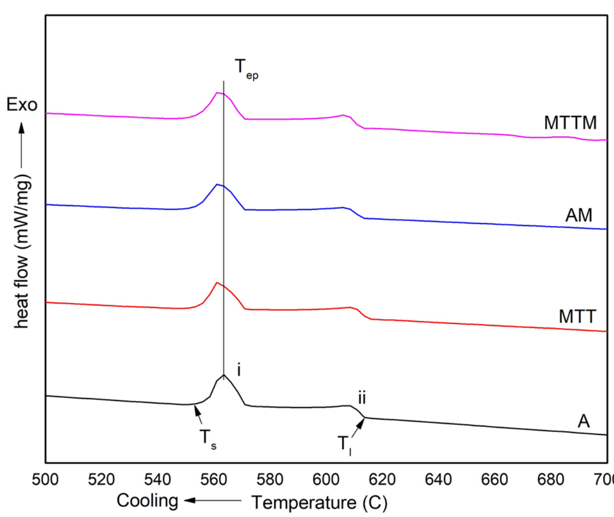

Fig. 4 DSC cooling curve of as-cast A356 alloys prepared by different treatments

Table 5 Variation in thermal parameters of as-cast A356 alloys treated in various ways

Sample	Liquidus temperature (°C)	Solidus temperature (°C)	Solidification range (°C)	Eutectic peak temperature (°C)
A	616.86	548.89	67.97	565.96
MTT	615.76	547.30	68.46	563.52
AM	616.96	546.86	70.1	561.06
MTTM	615.96	546.08	69.88	560.86

temperature) after the MTT process. The maximum solidification range is 70.1 °C in the case of the AM alloy. Zhang et al. [16] have concluded that the eutectic temperature and the freezing range become wider after adding Yb and La. These thermal analysis results justify the results of microstructural analysis that the addition of modifier along with MTT treatment can cause very significant modification in eutectic Si. Figure 5 shows DSC cooling curves of as-cast and aged MTT alloys. The results indicate that aging is not the cause of considerable variation in the cooling curve with respect to the as-cast alloys. This is because of the diminishing aging effect after remelting of aged alloys in DSC instruments.

Mechanical Properties

The variation in ultimate tensile strength (UTS), elongation, and Vickers hardness (VHN) of as-cast and aged A356 alloys is summarized in Fig. 6a–c. The results show that the properties are significantly increased after the aging process in each of the alloys. These enhancements are attributed to

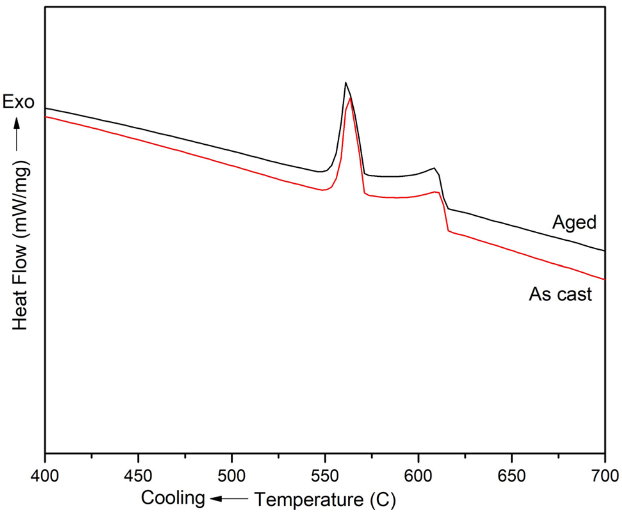

Fig. 5 DSC cooling curve of as-cast and aged MTT alloy

the spherodization of eutectic Si particles and the dissolution of Si and Mg in α-Al matrix [30]. The maximum variation in UTS after aging is observed in the aged A alloy, approximately 55.5% compared to the as-cast A alloy. The data obtained for different casting conditions of as-cast A356 alloy reveal that MTT process improves mechanical properties, especially ductility, with or without modifier compared to untreated alloy. This results from better grain refinement of α-Al and refinement of eutectic Si particles to a certain extent in the MTT process. The UTS, elongation, and VHN of as-cast MTTM alloys are increased by 18.6%, 38.8%, and 15.7%, respectively, compared to that of the as-cast A alloy and increased by 4.4%, 3.2%, and 2%, respectively, compared to that of the as-cast AM alloy. These results are justified by the research of Wang et al. [32]. They have concluded that the improvement in UTS of as-cast A356 alloy is limited, but the ductility increases by 46.2% after the MTT process. Jia et al. [22] have also reported that tensile strength and elongation increase

by 20.3% and 19.2%, respectively, by the melt thermal rate treatment, compared to that of the untreated Al–9Si–0.5 Mg alloy.

The variation in mechanical properties of different as-cast alloys can be described as follows. The size, shape, and distribution of eutectic Si particles along with the grain size of α-Al are important parameters that affect the value of impact energy of cast Al–Si alloys [36]. The alloy having more refined and uniformly distributed phases is expected to have higher strength properties. The as-cast unmodified alloys (A and MTT) consist of large grains of α-Al and needle-like eutectic Si particles in the microstructure (Fig. 2a–b). These needle-like Si particles act as stress concentration sites or preferred crack initiation sites in the α-Al matrix. Hence, the ductility of these alloys is lesser compared to Sr-modified

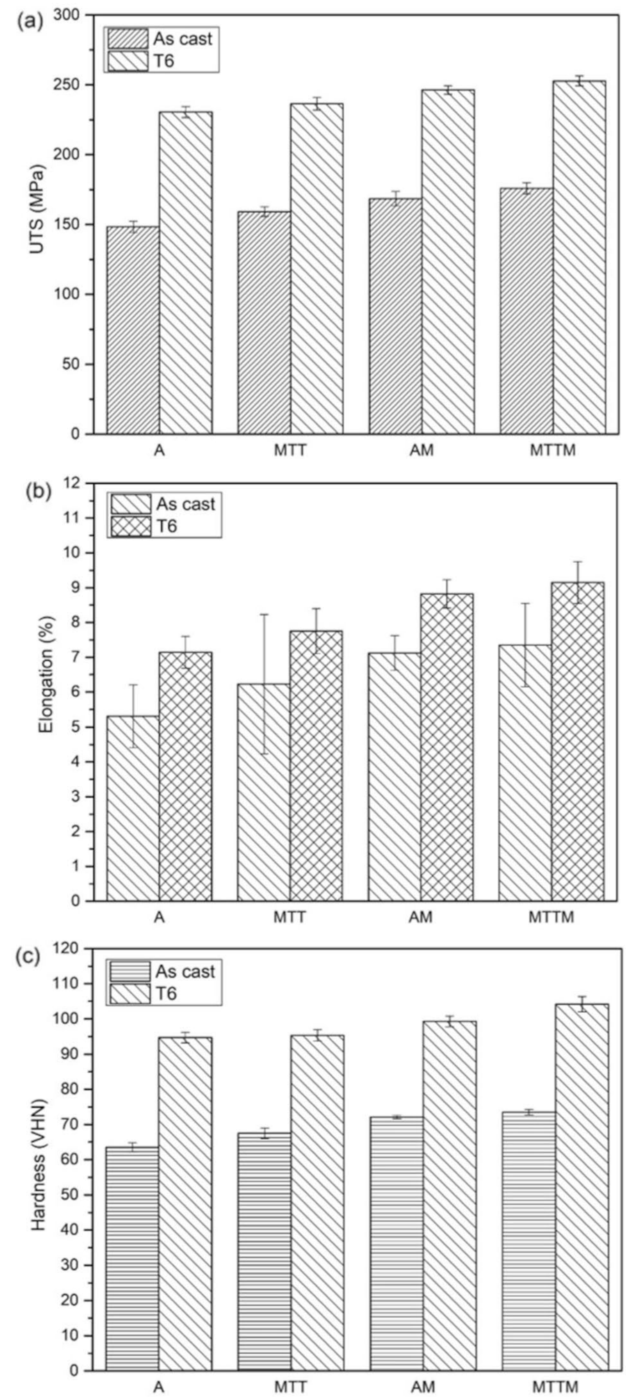

Fig. 6 Variations in mechanical properties of as-cast and aged A356 alloys **a** UTS, **b** elongation, and **c** hardness

alloys (AM and MTTM). The as-cast MTT alloy has a microstructure consisting of relatively finer α-Al grains and shorter needles of Si, and these features are responsible for better strength and ductility in MTT alloy over the A alloy. The morphology transformation in both Sr-modified alloys (AM and MTTM) leads to lower stress concentration effect of Si particles, and hence, Sr-modified alloys have better mechanical properties than unmodified alloys.

A similar trend is also found after aging treatment of various A356 alloys. The UTS, elongation, and VHN of aged MTTM alloy are increased by 9.6%, 24.4%, and 10.1%, respectively, compared to the aged A alloy, and increased by 2.6%, 3.7%, and 4.9%, respectively, compared to aged AM alloy. The variation in these properties is attributed to the morphology transition of eutectic Si, which depends on the size and shape of eutectic Si in the as-cast condition. The best modification in the morphology of eutectic Si is observed in the case of as-cast MTTM alloy, which results in better mechanical properties than other alloys. Ammar et al. [28] have also found that rapid enhancement in tensile properties after the aging process can be attributed to the change in Si particle morphology into round shape and dissolution of Mg and Si.

Fracture Analysis

SEM micrographs of fractured tensile test sample surfaces of various aged A356 alloys are shown in Fig. 7a–d and that of as-cast A356 alloy are shown in Fig. 6e. Each of the aged alloy fracture surfaces indicates a mixed mode of fracture (more dimple and less cleavage) because of the presence of modified morphology of eutectic Si. The modified alloys (both AM and MTTM) show small and uniformly distributed dimple structures compared to the unmodified alloys (A and MTT). This indicates that the ductility of modified alloys is better than that of the unmodified alloys, which justifies the tensile test results. The fracture surfaces of as-cast alloys fracture consist of cleavage planes due to the presence of longer needle-like eutectic Si which creates brittleness in the alloy.

The ductile fracture is dependent on the size of dimples or microvoids and the cracking behavior of eutectic Si [36]. In general, microvoids initiate the fracture as a result of decohesion of Si particles from the matrix (in modified alloys) or cracking of Si particles (in unmodified alloys). Then, coalescence of microvoids leads to the formation of microcracks followed by fracture. Small and perfectly spherical Si particles do not easily lead to decohesion/cracking compared to larger Si particles and less spherical particles. That is, why smaller and spherical eutectic Si in aged MTTM alloys

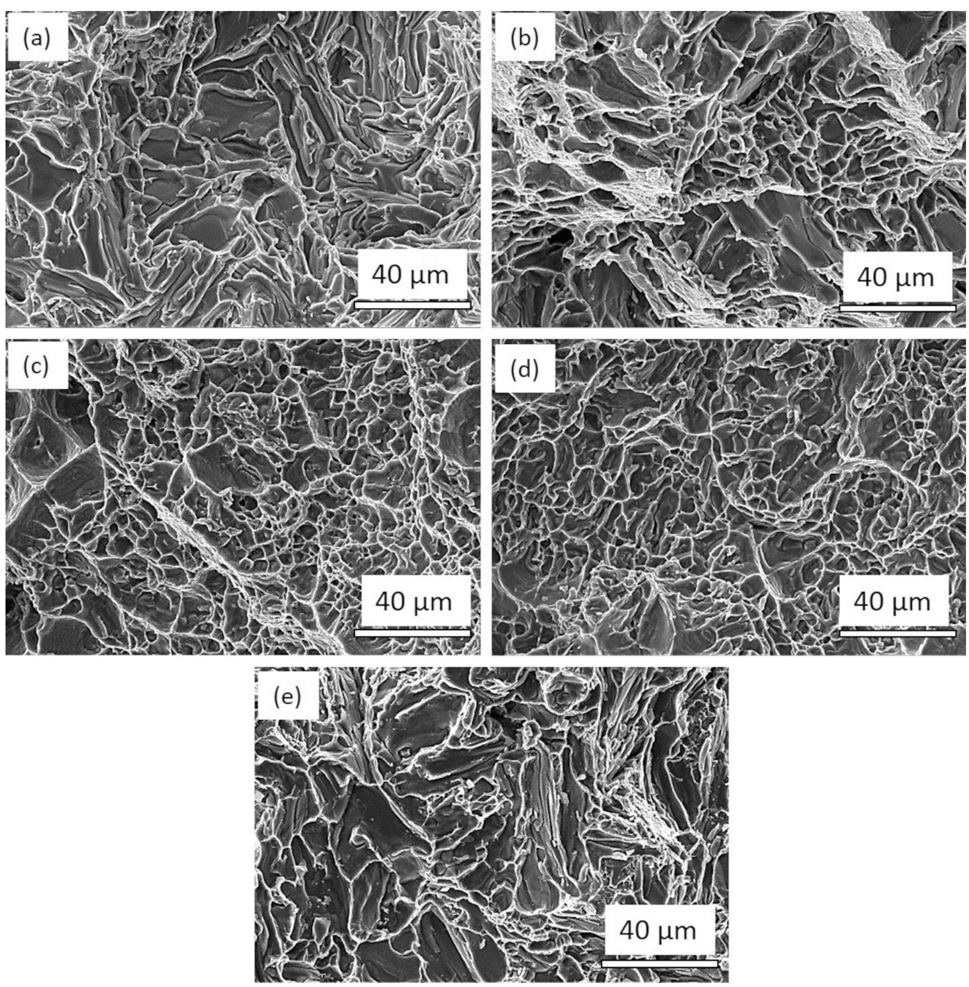

Fig. 7 SEM micrographs of fracture surfaces of aged A356 alloy **a** A, **b** MTT, **c** AM, **d** MTTM, and **e** as-cast A

provide better mechanical properties, specifically ductility, than other alloys.

Conclusions

The following conclusions can be made based on the present research:

1. Maximum reduction in grain size of α-Al and length of eutectic Si particles are observed in the case of as-cast MTTM alloy compared to other as-cast alloys.
2. Best modification in eutectic Si characteristic is found in aged modified alloys (AM and MTTM), and this is attributed to morphology transition into fibrous-like structure in the as-cast condition.
3. DSC analysis results have revealed that maximum eutectic peak temperature depression occurs in the case of MTTM alloys.
4. The rapid improvement in mechanical properties in the alloys after the aging process is because of the changes in the morphology of eutectic Si into spherical shape.
5. The maximum improvement in mechanical properties is observed in the MTTM alloy in both as-cast and aged conditions.

Acknowledgements The authors are thankful to TEQIP III, MNIT Jaipur, for providing financial assistance to carry out the research work.

References

1. S. Manani, P. Nikunj, A.K. Pradhan, Effect of modified casting process on toughness and wear resistance of LM25 alloy. Trans. Indian Inst. Met. **76**, 1095–1102 (2022)
2. S.L. Pramod, A.K. Prasada Rao et al., Effect of Sc addition and T6 ageing treatment on the microstructure modification and mechanical properties of A356 alloy. Mater. Sci. Eng. A. **674**, 438–450 (2016)
3. R. Gupta, A. Sharma, U. Pandel et al., Effect of heat treatment on microstructures and mechanical properties of A356 alloy cast through rapid slurry formation (RSF) process. Int. J. Cast Met. Res. **30**, 283–292 (2017)
4. S. Manani, A. Patodi, M.N. Verma et al., Comparative study of microstructure and properties of hypoeutectic Al–Si alloys being casted with and without melt thermal treatment. Metallogr. Microstruc. Anal. **11**, 415–424 (2022)
5. P.T. Li, S.D. Liu, L.L. Zhang et al., Grain refinement of A356 alloy by Al–Ti–B–C master alloy and its effect on mechanical properties. Mater. Des. **47**, 522–528 (2013)
6. S.K. Rathi, A. Sharma, M.D. Sabatino, Effect of mould temperature, grain refinement and modification on hot tearing test in Al-7Si-3Cu alloy. Eng. Fail. Anal. **79**, 592–605 (2016)
7. S.A. Kori, B.S. Murty, M. Chakraborty, Preparation and characterization of Al–B and B-rich Al–Ti–B master alloys for the grain refinement of Al–7Si alloy. AFS Trans. **109**, 267–286 (2001)
8. H. Li, T. Sritharan, Y.M. Lam et al., Effects of processing parameters on the performance of Al grain refinement master alloys Al–Ti and Al–B in small ingots. J. Mater. Process Technol. **66**, 253–257 (1997)
9. F. Taghavi, H. Saghafian, Y.H. Kharazi, Study on the effect of prolonged mechanical vibration on the grain refinement and density of A356 aluminium alloy. Mater. Des. **30**, 1604–1611 (2009)
10. G. Chirita, I. Stefanescu, D. Soares et al., Influence of vibration on the solidification behaviour and tensile properties of an Al–18 wt.%Si alloy. Mater. Des. **30**, 1575–1580 (2009)
11. J. Nampoothiri, I. Balasundar, B. Raj et al., Porosity alleviation and mechanical property improvement of strontium modified A356 alloy by ultrasonic treatment. Mater. Sci. Eng. A. **724**, 586–593 (2018)
12. A.M. Samuel, S.S. Mohamed, H.W. Doty et al., Grain refining of Al–Si alloys using Al-10% Ti master alloy: role of Zr addition. Int. J. Cast Met. Res. **32**, 46–58 (2019)
13. D. Qiu, J.A. Taylor, M.X. Zhang et al., A mechanism for the poisoning effect of silicon on the grain refinement of Al–Si alloys. Acta Mater. **55**, 1447–1456 (2007)
14. M. Zhu, Z.Y. Jian, L.J. Yao et al., Effect of mischmetal modification treatment on the microstructure, tensile properties, and fracture behaviour of Al–7.0%Si–0.3%Mg foundry aluminium alloys. J. Mater. Sci. **46**, 2685–2694 (2011)
15. Y. Dong, R. Zheng, X. Lin et al., Investigation on the modification behaviour of A356 alloy inoculated with a Sr–Y composite modifier. J. Rare Earths. **31**, 204–208 (2013)
16. S. Zhang, J. Leng, Z. Wang et al., Investigation on the modification behaviour of A356.2 alloy with Yb–La composite modifier. Mater. Res. Express. **5**, 016520 (2018). https://doi.org/10.1088/2053-1591/aaa657
17. A. Closset, J.E. Gruzleski, Structure and properties of hypoeutectic Al–Si–Mg alloys modified with pure strontium. Metall. Trans. A. **13**, 945–951 (1982)
18. T.F. Banamove, Superheating and refining. M Mech. **255c**, 112–123 (1965)
19. B. Xiufang, W. Weimin, Thermal-rate treatment and structure transformation of Al–13 Wt.% Si Alloy Melt. Mater. lett. **44**, 54–58 (2000)
20. Q. Wang, G. Haoran, Study of melt thermal-rate treatment and low-temperature pouring on Al- study of melt thermal-rate treatment and low-temperature pouring on Al-15 % Si alloy. J. Mater. **65**, 958–966 (2006)
21. Q. Wang, H.S. Geng, S. Zhang, Effects of melt thermal- rate treatment on Fe-containing phases in hypereutectic Al–Si alloy. Metall. Mater. Tran. A. **45**, 1621–1630 (2014)
22. P. Jia, J. Zhang, X. Hu et al., Grain refining effects of the melt thermal-rate treatment and Al–Ti–B–Y refiner in as-cast Al-9Si-05Mg alloy. Mater. Res. Express. **5**, 066520 (2018). https://doi.org/10.1088/2053-1591/aac994
23. A.M. Samuel, G.H. Garza-Elizondo, H. Doty et al., Role of modification and melt thermal treatment processes on the microstructure and tensile properties of Al–Si alloys. Mater. Des. **80**, 99–108 (2015)
24. M. Zhu, G. Yang, L. Yao et al., Effect of T6 heat treatment on the microstructures and the ageing behaviour of the grain-refined A356 alloys. Adv. Mat. Res. **143**, 1410–1414 (2010)
25. J. Chu, T. Lin, G. Wang et al., Effect of Heat Treatment on Microstructure and Properties of Al-7.0Zn-1.5Cu-1.5Mg-0.1Zr-0.1Ce Alloy. Metallogr. Microstruct. Anal. **9**, 312–322 (2020)
26. S.C. Ram, K. Chattopadhyay, I. Chakrabarty, Microstructures and high temperature mechanical properties of A356–Mg2Si functionally graded composites in as-cast and artificially aged (T6) conditions. J. Alloys Compd. **805**, 454–470 (2019)

27. H. Zhang, G. Chen, Z. Zhang et al., Study on the grain refinement of A356 alloy by Al–3 wt-% VN master alloy. Mater. Sci. Technol. **36**, 819–826 (2020)
28. H.R. Ammar, C. Moreau, A.M. Samuel et al., Effects of ageing parameters on the quality of 413-type commercial alloys. Mater. Des. **30**, 1014–1025 (2009)
29. N. Patel, S. Manani, A.K. Pradhan et al., Effect of solution heat treatment (temperature and time) on microstructure and properties of Al–Cu–Mg alloy. Int. J. Cast Met. Res. (2023). https://doi.org/10.1007/s40962-023-01095-6
30. F. Paray, J.J. Gruzleski, Modification-a parameter to consider in the heat treatment of Al–Si alloys. Cast Met. **5**, 187–198 (1993)
31. M. Zhu, Z. Jian, G. Yang, Effects of T6 heat treatment on the microstructure, tensile properties, and fracture behaviour of the modified A356 alloys. Mater. Des. **36**, 243–249 (2012)
32. J. Wang, S. He, B. Sun, Effects of melt thermal treatment on hypoeutectic Al–Si alloys. Mater. Sci. Eng. A. **338**, 101–107 (2002)
33. S.A. Al Kahtani, H.W. Doty, F.H. Samuel, Combined effect of melt thermal treatment and solution heat treatment on eutectic Si particles in cast Al–Si alloys. Int. J. Cast Met. Res. **27**, 38–47 (2014)
34. Z. Chen, C. Ma, P. Chen, Eutectic modification of A356 alloy with Li addition through DSC and Miedema model. Trans. Nonferrous Met. Soc. China. **22**, 42–46 (2012)
35. H.S. Kanga, W.Y. Yoon, K.H. Kim et al., Microstructure selections in the undercooled hypereutectic Al–Si alloys. Mater. Sci. Eng. A. **404**, 117–123 (2005)
36. Z. Ma, H.W. Doty, F.H. Samuel, On the Fractography of impact-tested samples of Al–Si alloys for automotive alloys, in *Fracture mechanics: properties, patterns and behaviors*. ed. by L. Alves (Intechopen science, London, 2016), pp.27–58